International Journal of Robotics and Control Systems
Vol. 2, No. 3, 2022, pp. 581-593
ISSN 2775-2658
http://pubs2.ascee.org/index.php/ijrcs

Active Control System Applied to Vibration Level Control in High-Speed Elevators

Marcos Gonçalves [a,1], Jose M. Balthazar [a,2], Clivaldo Oliveira [b,3], Maria E. K. Fuziki [c,4], Giane G. Lenzi [a,5], Angelo M. Tusset [a,6,*]

[a] Federal University of Technology – Paraná – Doutor Washington Subtil Chueire St., 330, Ponta Grossa – Paraná – 84017–220, Brazil
[b] Federal University of Grande Dourados – João Rosa Góes St., 1761, Vila Progresso – Dourados – Mato Grosso do Sul – 79825-070, Brazil
[c] State University of Maringá – Colombo Ave., 5790, Maringá – Paraná – 87020-900, Brazil
[1] marcos4036@hotmail.com; [2] jmbaltha@gmail.com; [3] ClivaldoOliveira@ufgd.edu.br; [4] mariafuziki@gmail.com; [5] gianeg@utfpr.edu.br; [6] tusset@utfpr.edu.br
* Corresponding Author

ARTICLE INFO

Article history
Received July 30, 2022
Revised August 20, 2022
Accepted September 05, 2022

Keywords
High-performance elevator;
Active control;
PID Control;
Vibration control

ABSTRACT

This work presents an active control system applied to vibration level reduction in high-performance vertical transport, aiming at improving the passengers' comfort in high-speed elevators. The control system design includes the use of a Proportional Integral Derivative (PID) control. Three strategies were proposed in order to achieve a 90% reduction in the vibration amplitudes: (I) the consecutive reduction of 90% of the displacements, (II) the consecutive reduction of 90% of the velocity, and (III) the consecutive reduction of 90% of the acceleration. The presentation of these three proposals allows their application for the use of different sensors. The performance of each strategy was evaluated through mathematical modeling and numerical simulations of a vertical transport with 4 degrees of freedom, submitted to excitations arising from rail deformations. Vibration and comfort levels in the cabin were numerically analyzed, taking into account ISO 2631 and BS 6841 standards for elevator lateral acceleration level and comfort level felt by passengers. Numerical simulations showed that the force required to reduce the vibration levels is practically the same for the three proposed strategies. However, strategy (III) – the successive reduction of 90% of acceleration – proved to be more efficient at improving passengers' comfort level when compared to the other two strategies.

1. Introduction

The current Civil Engineering technologies applied in the field of high-performance buildings and space utilization have collaborated for the development of new high-rise buildings, which demand the use of high-velocity elevators. The alternative movements of the elevator up and down the shaft during operation generate vibrations, causing discomfort to passengers [1-5]. In some cases, however, lateral vibration levels in the elevator cabin are so high that they can result in low comfort and reduced ride quality for the passengers, which are the main problems in high-speed elevator systems [6-10].

In [11-16], studies are presented that revealed that vibration during the elevator emergency braking process directly affects the performance of the elevator traction system, thus affecting the

safety, reliability, and comfort of passengers. In [17], results are presented that demonstrate that the vertical vibrations of the elevator traction system are maximized during the braking operation. In [18], it is shown that strong vibrations affect the contact force between the hoist rope and the traction sheave, consequently resulting in slipping between the hoist rope and the traction sheave.

In light of the need to improve its movement quality without losing the efficiency of the elevators within the limits of horizontal and vertical vibrations, research on control systems applied to the control of lateral and longitudinal accelerations has grown recently in order to guarantee the quality of passenger's ride [8]. In [7], active vibration control is proposed for a vertical transport model excited by the guide rail deformations considering the horizontal nonlinear response of the three degrees of freedom model. In [8], a design parameter optimization method is used to reduce the horizontal vibration of high-speed elevators. In [19-20], high-height lifting systems were studied, and the problem of the elevator rope with oscillating motion due to external force disturbances was also numerically studied through an active control, using non-linear controllers based on Lyapunov's theory to stabilize the cable swing. In [21], a model for the transverse vibrations of the elevator cable was presented. In [22], the investigation of a high-speed elevator system was considered, examining the horizontal vibrations caused by the guide "casters" in the elevator cabin. An active control system was proposed by [23] considering the time-varying states using the Co-FXLMS (Correlation Filtered-X Least-Mean-Square - Correlation Filter-X Minor Mean Square) and MBPF (Move Band Pass Filter - Motion Band Pass Filter).

In [24], an adaptive sliding-mode controller with diffuse switching gain (FGASMC) is proposed to reduce the severe horizontal vibration of the high-speed elevator car system that is caused by the excitation of the guide rail. In [25], an adaptive fuzzy-based sliding-mode predictive controller (PSMC-AF) is presented to reduce the horizontal vibration of the ultra-high-speed elevator car system. Numerical simulations are presented considering some representative excitations of the guide rail and demonstrated that the proposed active control is more effective than the passive system. In [26], a control system is proposed considering the combination of H_2/H_∞ to reduce the vibrations of the elevator cabin generated by the unevenness of the guide rail, uncertainty in the modeling of the guide shoe, wear and aging of the spring between the guide shoe bearing and guide rail. Numerical simulations demonstrated that the control strategy provided a better vibration suppression capability, significantly improving the lift displacement comfort.

In [27], the investigation of the non-linear mechanical problem of the elevator braking system under load and disturbance uncertainties from external excitation and its influence on driving comfort and on the operating efficiency of the elevator system is presented. In [28], the influence of the operating velocity of the high-speed elevator, the deviation of the guide rail profile, and the dynamic parameters of the rolling guide shoe on the horizontal vibration of the car in the comfort of passengers are presented. In [29], the authors presented a study about the lateral vibrations of suspension and compensation cables associated with the vertical movements of the cabin and the counterweight, which are induced by the movements of the building structure in high-rise elevators. In [30], the use of a magneto-rheological damper is considered a semi-active control to reduce the vibration levels of the high-speed elevator.

In [31], an investigation of the vibrations of the elevator cabin is carried out, considering the compensation cables and tension device in the vibration of the elevator, as well as the cabin and the lifting cables between the top of the cabin and the wheel. In [32], the damping characteristics of an elevator traction system are analyzed, and the vibration characteristics of the elevator cabin are tested considering a traction ratio of 2:1. Numerical results show that the natural frequency and stiffness of the system decrease with increasing elevator load and that the attenuation coefficient and damping increase with increasing elevator load, and the damping of the traction system is related to the initial direction of travel. In [33], a study of vertical vibrations caused by the ripple of torque generated in the elevator drive system and its influence on passenger comfort during an elevator ride was presented. In turn, [34] presented a methodology for the design of a high-performance LTI controller (Linear Time Invariant) by the vertical movement of the elevator with high velocity.

In [35], an SDRE control proposal was presented for the control of elevator cabin vibrations. Numerical results showed that the control strategy was efficient in reducing vibration levels. In [36], a mathematical model was presented considering the relationships of lateral force and tipping moment with horizontal displacement, deflection angle, and nominal velocity.

In works [37–39], a non-linear model of rolling guide shoes was proposed for the analysis of horizontal vibration responses considering the variation of parameters and irregularity of guide rails. In [40], the influence of cables on elevator vibration was studied. The proposed model was obtained by theoretical and experimental verification and applied to forecast the practical balances of buildings and elevator cables. In work [41], perturbation methods were applied, considering the derived defined and random part of the acceleration response expressions for analysis of the transverse vibration acceleration response.

The present work contributes to the body of knowledge on vibration control in high-speed elevators by presenting three different strategies for lateral vibration mitigation inside the elevator cabin. Unlike strategies that take into account lateral displacement or lateral velocity to control vibration, the present research approach was based on lateral acceleration control to determine the strong demand of the active control, facilitating its real implementation since it requires only accelerometers as sensors.

The paper is organized as follows: The introduction presents some of the most recent contributions to the research topic and the contribution of the present work to the body of knowledge. In the Method section, we present the mathematical model of the elevator cabin and the PID control project used to reduce lateral vibrations, considering the proposal of three strategies: consecutive reduction of 90% of displacements, consecutive reduction of 90% of the velocity, and the consecutive reduction of 90% of acceleration. The Results and Discussions section presents the numerical simulation results and the three different control strategies comparisons, taking into account the vibration levels according to ISO 2631 and BS 6841 standards. Finally, in the Conclusion, we present the conclusions of the results presented in the paper body.

2. Method

2.1. Mathematical Model

Fig. 1 represents a schematic diagram of the cabin elevator. The roller guides support the platform with springs to prevent transmission of external excitation caused by misalignment and deformation of the guide rollers. These guide rollers and springs are components of the suspension system.

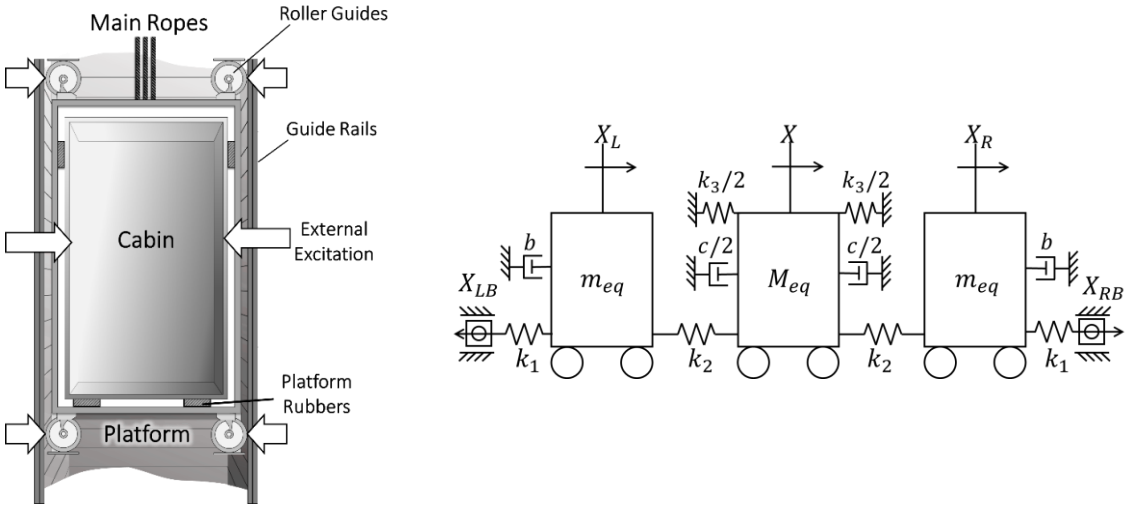

(a) (b)

Fig. 1. (a) Schematic diagram of elevator cabin structure (b) Equivalent model for the horizontal movement of the elevator

In Fig. 1, M_{eq} is cabin mass [kg]; m_{eq} is suspension system mass [kg]; b is suspension damping coefficient [Ns/m]; c is cabin damping coefficient [Ns/ m]; k_1 is stiffness coefficient of guide rollers [N/m]; k_2 is suspension stiffness coefficient [N/m]; k_3 is coefficient of stiffness of the elevator cables referring to the tilting movement of the cabin [N/m]; X is the horizontal displacement of the cabin [m]; X_L is a displacement of the left suspension system [m]; X_R is suspension system displacement to the right [m]; X_{LB} and X_{RB} are external excitations caused by deformations of the guide rails.

The motion equations can be obtained by using the Lagrange energy. Equation (1) represents the Euler-Lagrange equation.

$$\frac{d}{dt}\left[\frac{\partial L}{\partial \dot{q}_i}\right] - \frac{\partial L}{\partial q_i} = -Q_i, \qquad i = 1,2,3,\ldots,n \tag{1}$$

where q_i represents the generalized position coordinate; $\dot{q}_i$ represents the generalized velocity; L represents the Lagrange function, defined as the difference between the kinetic (T) and potential (V) energies of the system (2) [35].

Equation (2) shows the total kinetic energy of the system represented by Fig. 1, as the sum of the kinetic energies of the suspension systems, right and left, and the kinetic energy of the elevator cabin [12].

$$T = \frac{m_{eq}}{2}\dot{X}_L^2 + \frac{M_{eq}}{2}\dot{X}^2 + \frac{m_{eq}}{2}\dot{X}_R^2 \tag{2}$$

The total potential energy of the system is the sum of the potential energies of the spring elements with stiffness k_1, k_2 and k_3, referring, respectively, to the spring elements of the right and left suspension systems and of the translational spring element equivalent to the pendulum movement of the cab. That is, it represents the cabin, as shown in Equation (3) [35].

$$V = \frac{k_1}{2}(X_L - X_{LB})^2 + \frac{k_1}{2}(X_{RB} - X_R)^2 + \frac{k_2}{2}(X - X_L)^2 + \frac{k_2}{2}(X_R - X)^2 + \frac{1}{4}k_3X^4 \tag{3}$$

The conservative and non-conservative generalized forces of the system, Q_i, referring to the damping forces of the left and right suspension systems and the damping force of the cabin, which are represented by (4) [34].

$$Q_i = b\dot{X}_L + c\dot{X} + b\dot{X}_R \tag{4}$$

Using Lagrange's formulation, one can write the second-order differential Equations (5) that represent the vertical transport system as [7, 35]:

$$\begin{aligned} &m_{eq}\ddot{X}_L + b\dot{X}_L + (k_1 + k_2)X_L - k_2X = k_1X_{LB} \\ &M_{eq}\ddot{X} + c\dot{X} + 2k_2X + k_3X^3 - k_2X_L - k_2X_R = 0 \\ &m_{eq}\ddot{X}_R + b\dot{X}_R + (k_1 + k_2)X_R - k_2X = k_1X_{RB} \end{aligned} \tag{5}$$

Equation (5) can also be represented in the form of spaces as

$$\begin{aligned} \dot{x}_1 &= x_2 \\ \dot{x}_2 &= -\alpha_1x_2 - \alpha_2x_1 + \alpha_3x_3 + \alpha_4y_{left} \\ \dot{x}_3 &= x_4 \\ \dot{x}_4 &= -\sigma_1x_4 - \sigma_2x_3 - \sigma_3x_3^3 + \sigma_4x_1 + \sigma_5x_5 \\ \dot{x}_5 &= x_6 \\ \dot{x}_6 &= -\alpha_1x_6 - \alpha_2x_5 + \alpha_3x_3 + \alpha_4y_{right} \end{aligned} \tag{6}$$

where $x_1 = X_L, x_3 = X, x_5 = X_R, \alpha_1 = \frac{b}{m_{eq}}, \alpha_2 = \frac{(k_1+k_2)}{m_{eq}}, \alpha_3 = \frac{k_2}{m_{eq}}, \alpha_4 = \frac{k_1}{m_{eq}}, \sigma_1 = \frac{c}{M_{eq}}, \sigma_2 = \frac{2k_2}{M_{eq}}, \sigma_3 = \frac{k_3}{M_{eq}}, \sigma_4 = \frac{k_2}{M_{eq}}, \sigma_5 = \frac{k_2}{M_{eq}}$ and $y_{left} = y_{right} = a\,sin(\omega t)$.

2.2. Proposed Elevator Vibration Control System

The controller is integral state feedback. Fig. 2 shows the schematic diagram of the active control proposal.

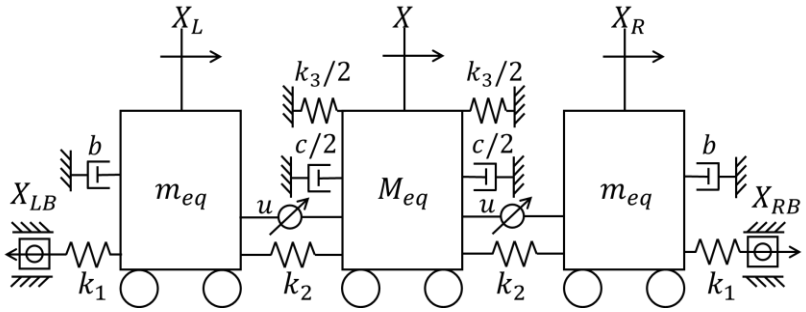

Fig. 2. Equivalent model for the horizontal movement of the elevator with active control

Equation (7) represents the horizontal movement of the elevator with a dynamic actuator, as shown in Fig. 2, and is given by:

$$\begin{aligned} m_{eq}\ddot{X}_L + b\dot{X}_L + (k_1 + k_2)X_L - k_2X &= k_1X_{LB} + u \\ M_{eq}\ddot{X} + c\dot{X} + 2k_2X + k_3X^3 - k_2X_L - k_2X_R &= -u \\ m_{eq}\ddot{X}_R + b\dot{X}_R + (k_1 + k_2)X_R - k_2X &= k_1X_{RB} + u \end{aligned} \tag{7}$$

Equation (7) can also be represented in the form of spaces:

$$\begin{aligned} \dot{x}_1 &= x_2 \\ \dot{x}_2 &= -\alpha_1x_2 - \alpha_2x_1 + \alpha_3x_3 + \alpha_4y_{left} + u \\ \dot{x}_3 &= x_4 \\ \dot{x}_4 &= -\sigma_1x_4 - \sigma_2x_3 - \sigma_3x_3^3 + \sigma_4x_1 + \sigma_5x_5 - u \\ \dot{x}_5 &= x_6 \\ \dot{x}_6 &= -\alpha_1x_6 - \alpha_2x_5 + \alpha_3x_3 + \alpha_4y_{right} + u \end{aligned} \tag{8}$$

where $\eta_1 = \frac{1}{m_{eq}}$ and $\eta_2 = \frac{1}{M_{eq}}$.

The state feedback control u is a PID controller and operates according to the block diagram in Fig. 3 where K_p is the proportional gain, K_d is the derivative gain and K_i is the corresponding integral gain of the control loop, respectively.

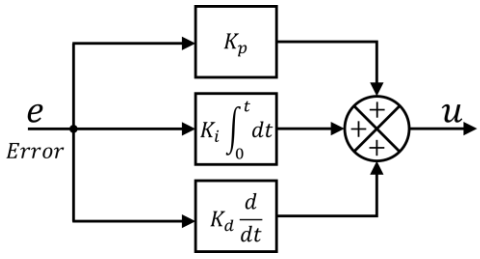

Fig. 3. Integral State Feedback Control System Block Diagram

The error used for the control by lateral displacement is given by $e = 0.9x_3$. The error used for velocity control is given by $e = 0.9\dot{x}_3$. And the error for the acceleration control is given by $e = 0.9\ddot{x}_3$. Fig. 4 shows the three different proposals presented in the paper.

In Fig. 4, we present the diagrams of the three control strategies investigated in this paper. Considering the numerical simulations of the system (8), the variables (x_3) and $(\dot{x}_3)$ are available in the system output. In a real application, the available states will depend on the sensor used. As can be seen in Fig. 4(a), the control signal u uses only the state (x_3) , in the vibration control, a state that represents the lateral displacement of the elevator car. In Fig. 4(b), the diagram for the control based

on the velocity ($\dot{x}_3$) of the lateral displacement of the cabin is presented. Fig. 4(c) shows the diagram for the control that uses lateral acceleration ($\ddot{x}_3$) of the cabin. For cases in which only displacement and lateral speed of the cabin are available, it is necessary to derive the lateral velocity ($\dot{x}_3$) once.

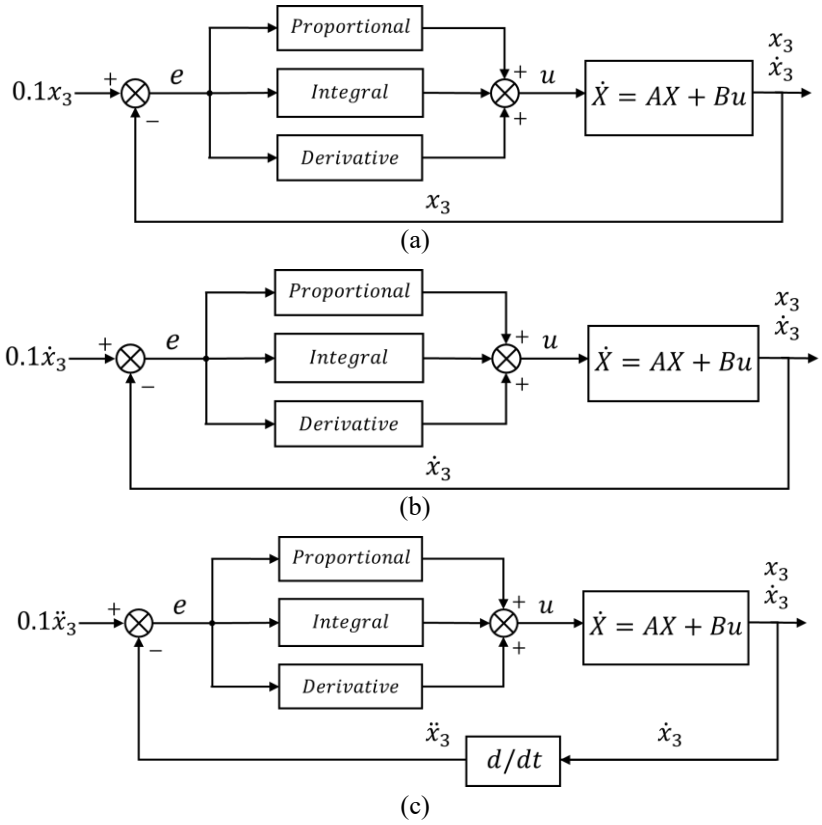

Fig. 4. Block diagram for PID control proposed: (a) control by lateral displacement of the cabin; (b) control by the velocity of lateral displacement of the cabin; (c) control by cabin lateral acceleration.

3. Results and Discussion

The numerical simulations were carried out taking into account the parameters described in Table 1 [7, 35]. In Fig. 5, it is possible to observe the variations in the displacement and acceleration levels that the cabin reaches without the introduction of active control.

Table 1. Parameters for numerical simulations

Parameters	Unit	Description	Value
M_{eq}	kg	Mass of the cabin	1120
m_{eq}	kg	Mass of the suspension system	17.5
b_1	N.s/m	Damping coefficient of the suspension	668.21
b_2	N.s/m	Damping coefficient of the cabin	2058.2
k_1	N/m	Stiffness coefficient of the guide rollers	250000
k_2	N/m	Stiffness coefficient of the suspension	19027
k_3	N/m	The stiffness coefficient of the spring is equivalent to the tilting motion of the cabin	1902700
a	m	External excitation amplitude	0.01
ω	rad/s	External excitation frequency	31.4159

To determine passenger comfort levels, the compensated acceleration (a_w) and estimated vibration dose value ($eVDV$) were considered in accordance with the following standards ISO 2631 and BS 6841 [42- 43].

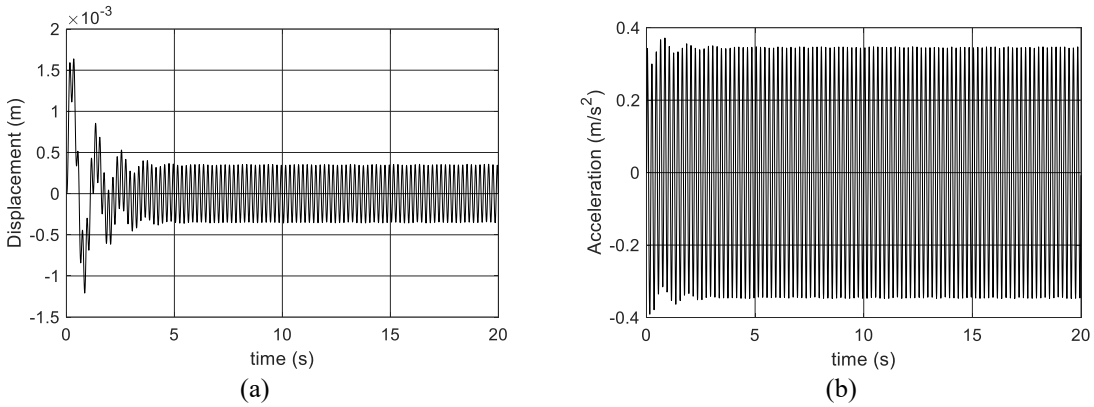

(a) (b)

Fig. 5. Elevator without active vibration control. (a) displacement. (b) acceleration

Compensated acceleration can be obtained from the Equation as

$$a_w = \left(\sum_i (W_i a_i)^2 \right)^{1/2} \tag{9}$$

where W_i is the compensation factor, and a_i is the acceleration in rms. Table 2 shows the compensation values used in a_w.

Table 2. Compensation values used in a_w

Frequency [Hz]	$W_k(\times 10^3)$	$W_k(\times 10^3)$	Frequency [Hz]	$W_k(\times 10^3)$	$W_k(\times 10^3)$
1	482	1011	10	988	212
1.25	484	1008	12.5	902	161
1.6	494	968	16	768	125
2	531	890	20	638	100
2.5	631	776	25	513	80
3.15	804	642	31.5	405	63.2
4	967	512	40	314	49.4
5	1039	409	50	246	38.8
6.3	1054	323	63	186	29.5
8	1036	253	80	132	21.1

The estimated vibration dose value ($eVDV$) was calculated by the following equation as

$$eVDV = \left(\left(1.4 a_{w_{rms}} \right)^4 \right)^{1/4} \tag{10}$$

where $eVDV$ represents the estimated vibration dose value [m/s$^{1.75}$], a_w represents the compensated acceleration according to direction, and in rms (m/s^2), and t the exposure time (seconds).

The level of exposure to vibration can also be estimated by calculating the root mean square (rms) as

$$rms = \sqrt{\left(\frac{1}{N} \sum {a_i}^2 \right)} \tag{11}$$

To determine the gains of the PID control, the Ziegler Nichols method and the use of the "Tuner" command of the *Simulink* were considered. The gains calculated for the PID control, considering the displacement control, were: $k_p = -2212575.41$, $k_d = -172909.07$ and $k_i = -2779520.02$. In Fig. 6, it is possible to observe the variations in the displacement and acceleration levels that the cabin reaches and the variation of the control signal. As can be seen in the results presented in Fig.

6, displacement control significantly reduced the acceleration and displacement of the cabin in comparison to the system without active control.

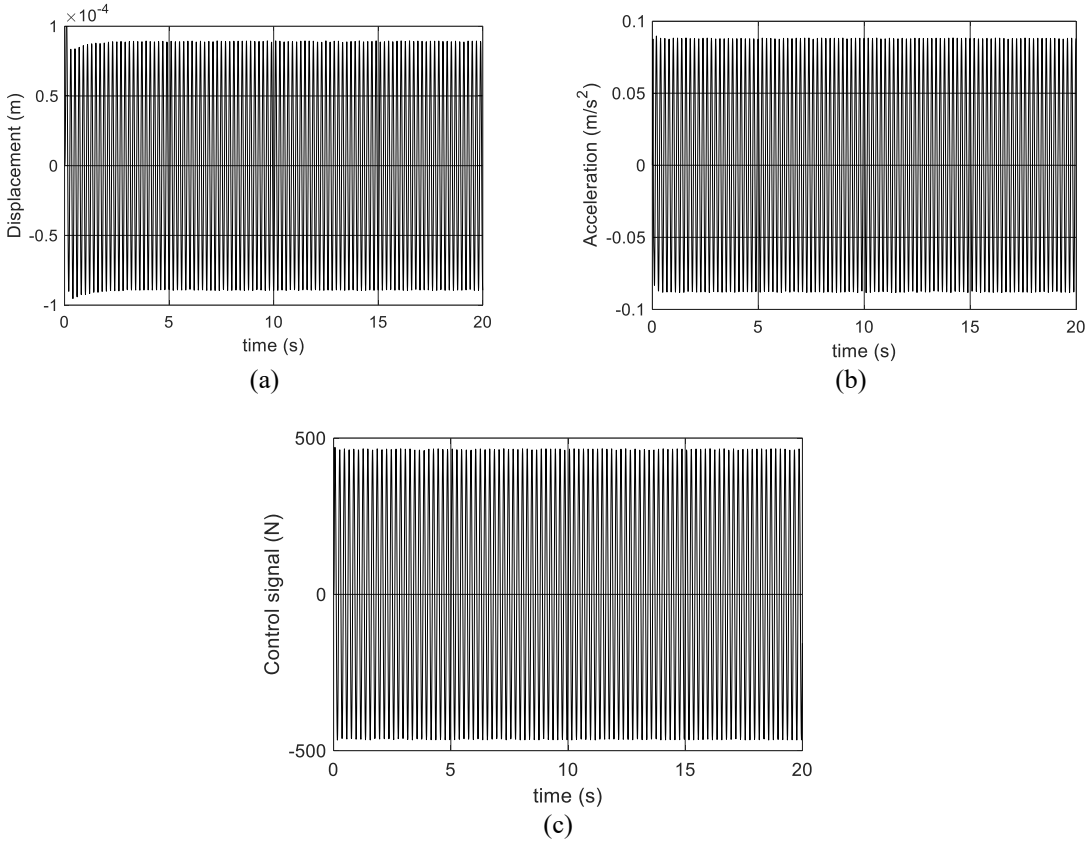

Fig. 6. PID control by displacement. (a) displacement. (b) acceleration. (c) control signal

The gains calculated for the PID control considering the velocity control were: $k_p = 801429.83$, $k_d = 10.42$ and $k_i = -148194505.47$. In Fig. 7, it is possible to observe the variations in the displacement and acceleration levels that the cabin reaches and the variation of the proposed control signal.

As can be seen in the results presented in Fig. 7, velocity control was more effective than displacement control in reducing acceleration and cabin displacement.

The gains calculated for the PID, considering the control by the acceleration, were given by: $k_p = 0$, $k_d = 0$ and $k_i = -5281537.69$. In Fig. 8, it is possible to observe the variations in the displacement and acceleration levels that the cabin reaches and the variation of the control signal.

As can be seen in the results presented in Fig. 8, acceleration control was more effective in reducing acceleration than displacement and velocity controls, but it was less efficient than velocity control in controlling displacement amplitudes. Considering passenger comfort as the objective, according to the numerical results presented, the control based on acceleration is the most recommended.

Fig. 9 shows the variations in the displacement and acceleration levels reached by the cabin and the variation of the control signal for the three strategies analyzed in this paper. As can be seen in Fig. 9(c), the three proposed control strategies used practically the same force amplitude in the control of lateral vibrations, demonstrating that an actuator can meet the demand of vibration control based on any of the three strategies.

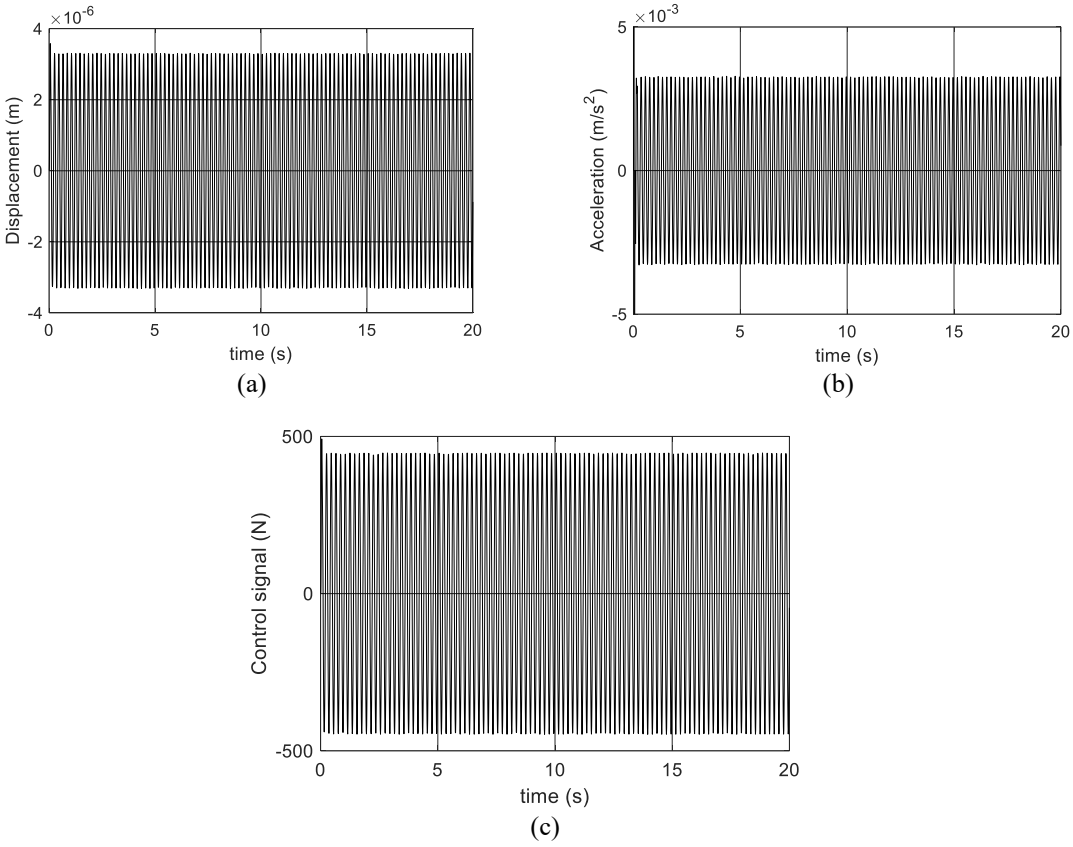

Fig. 7. PID control by velocity. (a) displacement. (b) acceleration. (c) control signal

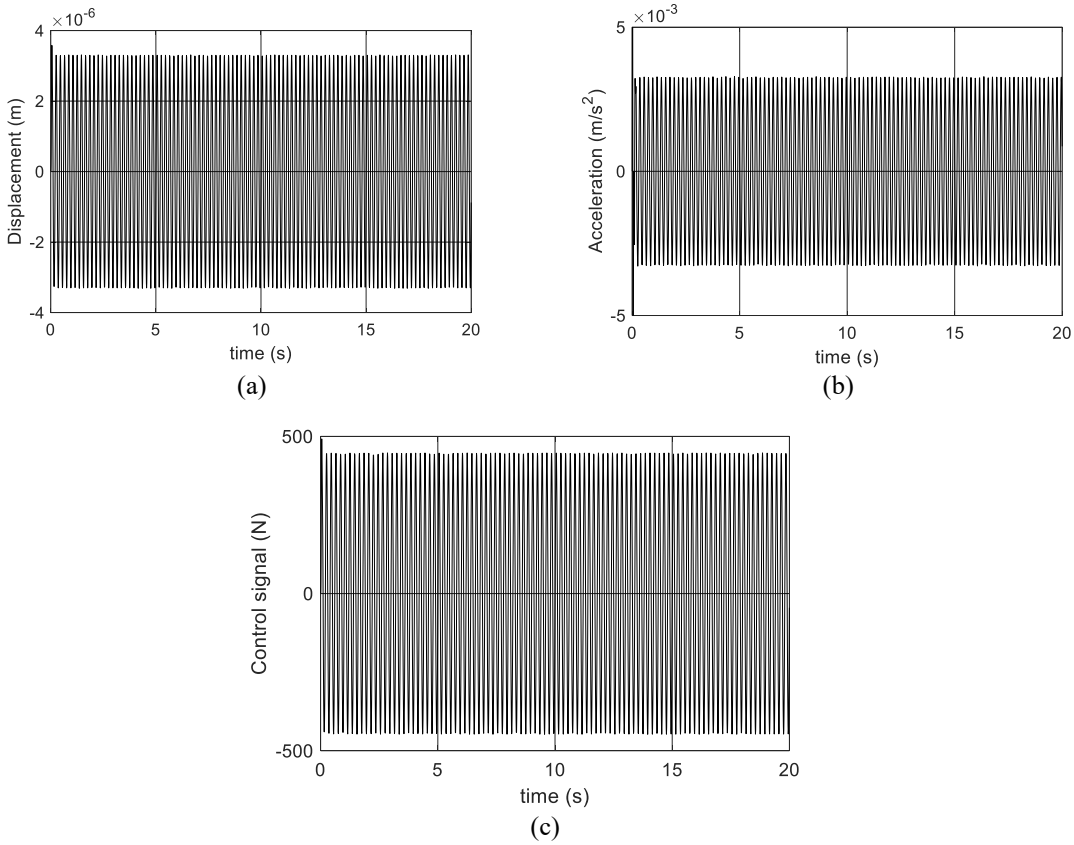

Fig. 8. PID control by acceleration. (a) displacement. (b) acceleration. (c) control signal

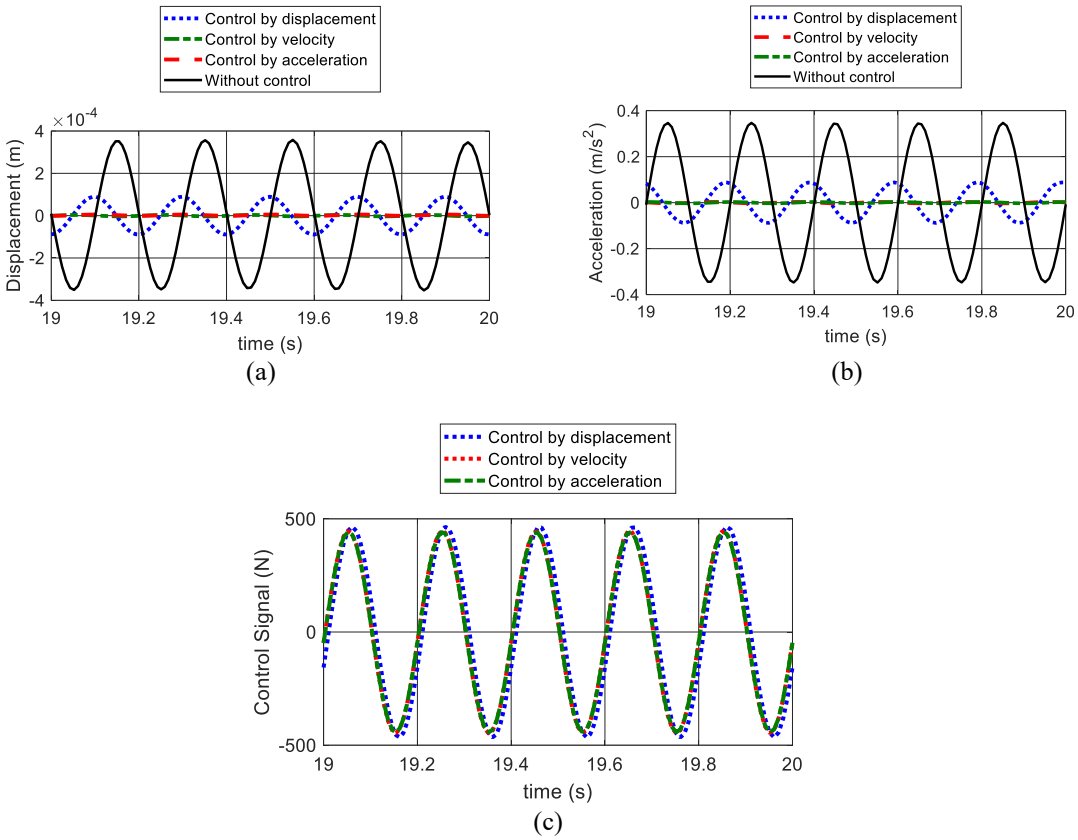

Fig. 9. PID control signals: (a) displacement, (b) acceleration, and (c) control.

Table 3 presents the main parameters to be considered in the analysis of control proposals. Considering the data presented in Table 3, the control strategy that allowed the best level of comfort for passengers was the control by acceleration.

Table 3. Analysis parameters of the proposed controls

Control /Results	Acceleration RMS (a_{RMS}) [m/s^2]	Compensated acceleration (a_w) [m/s^2]	Estimated vibration dose (eVDV) [$m/s^{1,75}$]	Range of displacement [m]
Control by acceleration	0.002064	0.000844	0.002499	0.0000063
Control by velocity	0.002343	0.000958	0.002837	0.0000068
Control by displacement	0.062009	0.025361	0.075087	0.000204
No control	0.242328	0.099112	0.293435	0.002846

4. Conclusion

The numerical results presented showed that the active control strategy that allowed the best passengers' comfort level was the control by acceleration. The control by acceleration presented approximately a 99.1% reduction of the acceleration RMS, resulting from the proposed strategy that considers a 90% reduction of the acceleration in the controlled system.

As can be seen in Table 3, control strategies that use acceleration or velocity as control parameters significantly reduced displacement to levels below the 10% considered for control by displacement.

It can also be seen in Table 3 that the reduction in acceleration RMS for acceleration-based control was approximately 99.1%. For displacement control, the reduction was approximately 74.41%.

The advantage of applying the PID control strategy using the acceleration variation, in comparison to other strategies, such as the SDRE proposed in [35], and the LQR proposed in [7], for example, is that the control by the acceleration proposed in this paper, we can get the signal directly from the sensor (accelerometer), without the need to integrate twice to get displacement and position, which is necessary for SDRE control and LQR control.

In future works, the use of a magnetorheological damper to control vibration will be considered. The current to be applied to the damper coil is determined according to the force estimated by the PID control proposed in this paper, a strategy similar to that presented in [7].

Author Contribution: All authors contributed equally to the main contributor to this paper. All authors read and approved the final paper.

Funding: This research received no external funding.

Acknowledgment: The authors acknowledge the CAPES, FAPESP, FA, and CNPq, both Brazilian research funding agencies.

Conflicts of Interest: The authors declare no conflict of interest.

References

[1] L. Hrabovský, T. Mlcak, and G. Kotajny, "Forces generated in the parking brake of the pallet locking system," *Adv. Sci. Technol. Res. J.*, vol. 13, no. 4, pp. 181–187, 2019, https://doi.org/10.12913/22998624/111478.

[2] Q. Peng, Z. Li, H. Yuan, G. Huang, S. Li, and X. Sun, "A model-based unloaded test method for analysis of braking capacity of elevator brake," *Adv. Sci. Technol. Res. J.*, vol. 2018, 2018, https://doi.org/10.1155/2018/8047490.

[3] T. X. Nguyen, N. Miura, and A. Sone, "Analysis and control of vibration of ropes in a high-rise elevator under earthquake excitation," *Earthq. Eng. Eng. Vib.*, vol. 18, no. 2, pp. 447–460, 2019, https://doi.org/10.1007/s11803-019-0514-9.

[4] S. Cao, R. Zhang, S. Zhang, S. Qiao, D. Cong, and M. Dong, "Roller-rail parameters on the transverse vibration characteristics of super-high-speed elevators," *Transactions of the Canadian Society for Mechanical Engineering*, vol. 43, no. 4, pp. 535–543, 2019, https://doi.org/10.1139/tcsme-2018-0083.

[5] Q. Zhang, T. Hou, H. Jing, and R. Zhang, "Analysis of Longitudinal Vibration Acceleration Based on Continuous Time-Varying Model of High-Speed Elevator Lifting System with Random Parameters," *Mechanics & Industry*, vol. 22, pp. 28, 2021, https://doi.org/10.1051/meca/2021027.

[6] N. Mitsui and T. Nara, "Analysis of Horizontal Quaking of High-Speed Elevators," Hitachi Rev, vol. 20, no. 8, pp. 342–348. 1971.

[7] A. M. Tusset, D. R. Santo, J. M. Balthazar, V. Piccirillo, L. C.C. Dos Santos, and R. M.L.R.F. Brasil, "Active Vibration Control of an Elevator System Using Magnetorheological Damper Actuator," *Int. J. Nonlinear Dyn. Control*, vol. 1, no 1, pp. 114–131, 2017, https://doi.org/10.1504/IJNDC.2017.083642.

[8] L. Qiu, Z. Wang, S. Zhang, L. Zhang, and J. Chen, "A Vibration-Related Design Parameter Optimization Method for High-Speed Elevator Horizontal Vibration Reduction," *Shock Vib.*, vol. 2020, pp. 1–20, 2020, https://doi.org/10.1155/2020/1269170.

[9] L. Qiu, G. Su, Z. Wang, S. Zhang, L. Zhang, and H. Li, "High-speed elevator car horizontal vibration fluid-solid interaction modeling method," J. Vib. Control, vol. 4, pp. 1–17, 2021, https://doi.org/10.1177/10775463211023361.

[10] N. Wang, G. Cao, L. Yan, and L. Wang, "Modelling and passive control of flexible guiding hoisting system with time-varying length," *Mathematical and Computer Modelling of Dynamical Systems*, vol. 26, no. 1, pp. 31–54, 2020, https://doi.org/10.1080/13873954.2019.1699121.

[11] P. Lonkwic, T. Krakowski, and H. Ruta, "Application of stray magnetic field for monitoring the wear degree in steel components of the lift guide rail system," *Metals*, vol. 10, no. 8, pp. 1008, 2020, https://doi.org/10.3390/met10081008.

[12] Z. Li, H. Ma, P. Xu, Q. Peng, G. Huang, and Y. Liu, "Prediction Model and Experimental Study on Braking Distance under Emergency Braking with Heavy Load of Escalator," *Mathematical Problems in Engineering*, vol. 2020, 2020, https://doi.org/10.1155/2020/7141237.

[13] A. Wu, X. Shi, L. Weng, and D. Hu, "Thermo-mechanical modeling and transient analysis of frictional braking of elevator safety gear," *Journal of Thermal Stresses*, vol. 43, no. 12, pp. 1467–1486, 2020, https://doi.org/10.1080/01495739.2020.1820921.

[14] X. Ma, G. Pan, P. Zhang, Q. Xu, X. Shi, Z. Xiao, and Y. Han, "Experimental Evaluation of Braking Pad Materials Used for High-Speed Elevator," *Wear*, vol. 477, 2021, https://doi.org/10.1016/j.wear.2021.203872.

[15] Q. Peng, A. Jiang, H. Yuan, G. Huang, S. He, and S. Li, "Study on Theoretical Model and Test Method of Vertical Vibration of Elevator Traction System," *Mathematical Problems in Engineering*, vol. 2020, 2020, https://doi.org/10.1155/2020/8518024.

[16] Q. Peng, P. Xu, Y. Li, H. Yuan, Z. Xue, and J. Yang, "Experiment Research on Emergency Stop Vibrations of Key Components in the Friction Vertical Lifting System," *Shock Vib*., 7816270, 2022, https://doi.org/10.1155/2022/7816270.

[17] S. Watanabe and T. Okawa, "Vertical vibration of elevator compensating sheave due to brake activation of traction machine," *Journal of Physics: Conference Series*, vol. 1048, no. 1, pp. 1–7, 2018, https://doi.org/10.1088/1742-6596/1048/1/012012.

[18] C. Webb and M. A. Tuck, "Cable disc elevator: static friction investigation," *Mining, Metallurgy & Exploration*, vol. 38, no. 2, pp. 979–994, 2021, https://doi.org/10.1007/s42461-020-00358-8.

[19] S. Kaczmarczyk and S. Mirhadizadeh, "Modelling, Simulation and Experimental Validation of Nonlinear Dynamic Interactions in an Aramid Rope System," *Appl. Mech. Mater*., vol. 706, pp. 117–127. 2014, https://doi.org/10.4028/www.scientific.net/AMM.706.117.

[20] M. Benosman and D. Fukui, "Lyapunov-Based Control of the Sway Dynamics for Elevator Ropes," In 2014 American Control Conference, pp. 329–334, 2014, https://doi.org/10.1109/ACC.2014.6858585.

[21] S. H. Sandilo and W. T. van Horssen, "On a Cascade of Auto resonances in an Elevator Cable System," *Nonlinear Dyn*., vol. 80, no. 3, pp. 1613–1630. 2015, https://doi.org/10.1007/s11071-015-1966-8.

[22] C.-C. Chang, C.-C. Lin, W.-C. Su, and Y.-P Huang, "H∞ Direct Output Feedback Control of High-Speed Elevator Systems," *Seismic Engineering; ASMEDC*, vol. 8, pp 289–296, 2011, https://doi.org/10.1115/PVP2011-57814.

[23] S. Yang and M. Lynn," More Evidence Challenging the Robustness and Usefulness of the Attraction Effect," *J. Mark. Res*., vol. 51, no. 4, pp. 508–513, 2014, https://doi.org/10.1509/jmr.14.0020.

[24] Q. He, T. Jia, R. Zhang, and L. Liu, "Adaptive sliding mode control with fuzzy adjustment of switching term based on the Takagi-Sugeno model for horizontal vibration of the high-speed elevator cabin system," *Proc. Inst. Mech. Eng. Part C J. Mech. Eng. Sci*., vol. 236, no. 9, pp. 4503-4519, 2022, https://doi.org/10.1177/09544062211053191.

[25] H. Wang, M. Zhang, R. Zhang, and L. Liu, Research on predictive sliding mode control strategy for horizontal vibration of ultra-high-speed elevator car system based on adaptive fuzzy. *Measurement and Control*, vol. 54, no. (3-4), pp. 360-373. 2021, https://doi.org/10.1177/00202940211003926.

[26] C. Chen, R. Zhang, Q. Zhang, and L. Liu, "Mixed H_2/H_∞ guaranteed cost control for high speed elevator active guide shoe with parametric uncertainties," *Mechanics & Industry*, vol. 21, no. 5, pp. 502, 2020, https://doi.org/10.1051/meca/2020044.

[27] P. Wolszczak, P. Lonkwic, and J. A. Cunha, "Robust optimization and uncertainty quantification in the nonlinear mechanics of an elevator brake system," *Meccanica*, vol. 54, pp. 1057–1069, 2019, https://doi.org/10.1007/s11012-019-00992-7.

[28] L. Qiu, G. Su, Z. Wang, S. Zhang, L. Zhang, H. Li, "High-speed elevator car horizontal vibration fluid–solid interaction modeling method," *J. Vib. Control*, 2021, https://doi.org/10.1177/10775463211023361.

[29] R. S. Crespo, S. Kaczmarczyk, P. Picton, and H. Su, "Modelling and simulation of a stationary high-rise elevator system to predict the dynamic interactions between its components," *International Journal of Mechanical Sciences*, vol. 137, pp. 24–45. 2018, https://doi.org/10.1016/j.ijmecsci.2018.01.011.

[30] Z. Wang, L. Qiu, S. Zhang, G. Su, L. Zhu, and X. Zhang, "High-speed elevator car system semi-active horizontal vibration reduction method based on the improved particle swarm algorithm," *J. Vib. Control*, 2022, https://doi.org/10.1177/10775463221089425.

[31] Q. Hang, Y. Yang, T. Hou, and R. Zhang, "Dynamic analysis of high-speed traction elevator and traction car–rope time-varying system," *Noise & Vibration Worldwide*, vol. 50, no. 2, pp. 37-45, 2019, https://doi.org/10.1177/0957456519827929.

[32] P. Xu, Q. Peng, F. Jin, F. Xia, J. Xue, H. Yuan, and S. Li, "Experimental study on damping characteristics of elevator traction system," *Advances in Mechanical Engineering*, 2022, https://doi.org/10.1177/16878132221085434.

[33] X. Arrasate, S. Kaczmarczyk, G. Almandoz, J. M. Abete, and I. Isasa, "The Modelling, Simulation and Experimental Testing of the Dynamic Responses of an Elevator System," *Mech. Syst. Signal Process*, vol. 42, no. (1–2), pp. 258–282. 2014, https://doi.org/10.1016/j.ymssp.2013.05.021.

[34] S. R. Venkatesh, Y. M. Cho, and J. Kim, "Robust Control of Vertical Motions in Ultra-High Rise Elevators," *Control Eng. Pract*., vol. 10, no. 2, pp. 121–132. 2002, https://doi.org/10.1016/S0967-0661(01)00111-3.

[35] D. Santo, J. Balthazar, A. Tusset, V. Piccirilo, R. Brasil, and M. Silveira, "On Nonlinear Horizontal Dynamics and Vibrations Control for High-Speed Elevators," *J. Vib. Control*, vol. 24, no. 5, pp. 825–838, 2016, https://doi.org/10.1177/1077546316667324.

[36] J. Liu, R. Zhang, Q. He, and Q. Zhang, "Study on Horizontal Vibration Characteristics of High-Speed Elevator with Airflow Pressure Disturbance and Guiding System Excitation," *Mech. Ind*., vol. 20, no. 3, 2019, https://doi.org/10.1051/meca/2019013.

[37] R. Zhang, C. Wang, Q. Zhang, and J. Liu, "Response Analysis of Non-Linear Compound Random Vibration of a High-Speed Elevator," *J. Mech. Sci. Technol*., vol. 33, no. 1, pp. 51–63. 2019, https://doi.org/10.1007/s12206-018-1206-5.

[38] R. Zhang, C. Wang, and Q. Zhang, "Response Analysis of the Composite Random Vibration of a High-Speed Elevator Considering the Nonlinearity of Guide Shoe," *J. Brazilian Soc. Mech. Sci. Eng*., vol. 40, no. 4, 2018, https://doi.org/10.1007/s40430-017-0936-0.

[39] Q. Zhang, Z. Yang, C. Wang, Y. Yang, and R. Zhang, "Intelligent Control of Active Shock Absorber for High-Speed Elevator Car," *Proc. Inst. Mech. Eng. Part C J. Mech. Eng. Sci*., vol. 233, no. 11, pp. 3804–3815, 2019, https://doi.org/10.1177/0954406218810045.

[40] D.-H. Yang, K.-Y. Kim, M. K. Kwak, and S. Lee, "Dynamic Modeling and Experiments on the Coupled Vibrations of Building and Elevator Ropes," *J. Sound Vib*., vol. 390, pp. 164–191. 2017, https://doi.org/10.1016/j.jsv.2016.10.045.

[41] C. Wang, R. Zhang, and Q. Zhang, "Analysis of Transverse Vibration Acceleration for a High-Speed Elevator with Random Parameter Based on Perturbation Theory," *Int. J. Acoust. Vib*., vol. 22, no. 2, pp. 2018-2023, 2017, https://doi.org/10.20855/ijav.2017.22.2467.

[42] British Standard Guide. BS 6841: Measurement and Evaluation of Human Expo-Sure to Whole-Body Mechanical Vibration and Repeated Shock, 1987.

[43] ISO Standard. ISO 2631-1: Mechanical Vibration and Shock – Evaluation of Human Exposure to Whole-Body Vibration – Part I: General Requirements, 1997.